Vol 17 No 8, August 2008
1674-1056/2008/17(08)/2890-07

Chinese Physics B

© 2008 Chin. Phys. Soc.
and IOP Publishing Ltd

Calculations of state-selective differential cross sections for charge transfer in collisions between O^{3+} and H_2*

Chi Bao-Qian(迟宝倩)[a], Liu Ling(刘 玲)[b], and Wang Jian-Guo(王建国)[b]

[a] *College of Science, Shenyang Science and Technology University, Shenyang* 110168, *China*

[b] *Institute of Applied Physics and Computational Mathematics, Beijing* 100088, *China*

(Received 20 February 2008; revised manuscript received 27 March 2008)

The non-dissociative charge-transfer processes in collisions between O^{3+} and H_2 are investigated by using the quantum-mechanical molecular-orbital coupled-channel (QMOCC) method. The adiabatic potentials and radial coupling matrix elements utilized in the QMOCC calculations are obtained with the spin-coupled valence-bond approach. Electronic and vibrational state-selective differential cross sections are presented for projectile energies of 0.1, 1.0 and 10.0 eV/u in the H_2 orientation angles of 45° and 89°. The electronic and the vibrational state-selective differential cross sections show similar behaviours: they decrease as the scattering angle increases, and beyond a specific angle the oscillating structures appear. Moreover, it is also found that the vibrational state-selective differential cross sections are strongly orientation-dependent, which provides a possibility to determine the orientations of molecule H_2 by identifying the vibrational state-selective differential scattering processes.

Keywords: charge transfer, molecular-orbital coupled-channel method, infinite-order sudden approximation, state-selective differential cross sections

PACC: 2570, 8230F

1. Introduction

Charge transfer processes occurring in collisions between ions and neutral atoms and between ions and molecules are still one of the most important research fields in atomic and molecular physics. This interest stems not only from fundamental aspects involved, but also from their importance in astrophysical and laboratory plasmas. Charge transfer provides a recombination mechanism for multiply charged ions in x-ray ionized astrophysical environments with low electron densities.[1] For example, it has been found that the extreme ultraviolet (EUV) and x-ray emission from comets and planetary atmospheres result from charge transfer between highly charged solar wind ions and cometary neutral molecules.[2,3] In the divertor region of a tokamak fusion device, charge exchanges between impurity ions and neutral atoms and between ions and molecules play an important role in the ionization balance and the production of radiative energy loss leading to cooling.[4,5] In inertial confinement fusion (ICF) research, recent experiments indicate that charge transfer is needed to explain some unusual high-intensity silicon spectra in a high-density and high-temperature plasma.[6,7] In order to model and understand the behaviours in these environments, it is necessary to obtain the total, state-selective and differential cross sections or rate coefficients. Numerous experimental and theoretical studies have been performed for ion-molecule collisions.[8−12] However, to our knowledge, few reports on state-selective differential cross sections are available.

The molecular hydrogen is one of the most primary ingredients in the planetary atmospheres, so the charge-transfer process between multiply charged ions with H_2 is of particular significance. In a previous paper,[13] the non-dissociative charge-transfer process in collisions between O^{3+} and H_2 ($v = 0$) has been investigated: the state-selective cross sections are calculated for the final states H_2^+ (v') with the values of vibrational quantum number $(v)' \leq 9$ and the dependences of cross section on orientation of H_2 molecules are analysed. But as is well known, the differential scattering cross section should be much more sensitive

*Project supported by the National Natural Science Foundation of China (Grant Nos 10574018 and 10574020).

to orientation, therefore, it is possible to develop a new diagnostic method to determine the molecular orientations. In the work of Wu *et al*,[14] they have found the strong dependence of differential scattering cross section on orientation by using the quantum-mechanical molecular-orbital coupled-channel (QMOCC) method in the vibrational sudden approximation. The vibrational sudden approximation cannot hold at low energies ($< 100\,\mathrm{eV}$), but the effects of molecular orientations should be more prominent at the low energies, for the low-energy collision is more dependent on the detail of molecule structure.

In the present work, all the vibrational bound states of $H_2^+(v')$ are considered in the following reaction:

$$\begin{aligned} &O^{3+}(2s^2 2p^2 P^0) + H_2(1s^2 X^1\Sigma_g^+) \\ &\rightarrow O^{2+}(2s^2 2p3s^{1,3}P^0) + H_2^+(1sX^2\Sigma_g^+) \end{aligned} \quad (1)$$

by using the QMOCC method in the infinite-order sudden approximation. In the infinite-order sudden approximation, we can calculate the charge transfer processes at lower energies until to $0.1\,\mathrm{eV/u}$.[12,13] For the initial channel, similar to those in Ref.[13] and available experiments,[15−20] only the ground state of H_2 is considered. Besides the total, electronic and vibrational state-selective cross sections, we also calculate the state-selective differential cross sections at the low energies.

In the QMOCC calculations, the adiabatic potentials and radial coupling matrix elements in Ref.[13] for various orientations are utilized, which have been calculated by using the spin-coupled valence-bound (SCVB) method. The orientation is specified by an angle θ, which is defined as the angle between the H-H diatom nuclear vector $\boldsymbol{r}$ and the internuclear radius vector $\boldsymbol{R}$ from the centre of mass of H_2 to oxygen ion. The molecular data are calculated for $R = (3-13)\,a_0$ and the values of r being 1.2, 1.4, 1.6 and $2.0\,a_0$, where the equivalent distance for ground state of H_2 is equal to $1.4\,a_0$. In the same way as in Ref.[13], the rotational motion of H_2 molecule is not taken into account, so the values of angle θ are taken as constants of 45° and 89° in the calculations. In Section 2 we review the scattering theory used in the present calculations. The results and discussion are presented in Section 3 and a brief conclusion is given in Section 4. Unless otherwise stated, atomic units are used throughout the paper.

2. Scattering theory

The QMOCC method is used in our calculations in the infinite order sudden approximation.[12,13] The infinite order sudden approximation is appropriate when the rotational periods of molecules are much longer than the collision time. In the centre-of-mass coordinate system, the Hamiltonian of the collision system can be represented by

$$\begin{aligned} H(R, r, \rho_i) = &-\frac{1}{2\mu_R}\nabla_R^2 - \frac{1}{2\mu_r}\nabla_r^2 \\ &+ H_{\mathrm{ad}}(\rho_i|R, r), \end{aligned} \quad (2)$$

where μ_R is the reduced mass of the collision system, μ_r the reduced mass of H_2 molecule, ρ_i the electronic coordinate, and H_{ad} the adiabatic electronic Hamiltonian of the triatomic molecular ion $[OH_2]^{3+}$. The Schrödinger equation for the adiabatic Hamiltonian is then

$$\begin{aligned} &H_{\mathrm{ad}}(\rho_i|R, r)\phi_\gamma(\rho_i|R, r) \\ &= \varepsilon_\gamma(R, r, \theta)\phi_\gamma(\rho_i|R, r), \end{aligned} \quad (3)$$

where $\varepsilon_\gamma(R, r, \theta)$ and $\phi_\gamma(\rho_i|R, r)$ are the triatomic adiabatic electronic energy and the wave function of the ion-molecule system, respectively. Within the perturbed stationary-state (PSS) approximation, total wave function for the ion-molecule system can be expanded over a complete basis of adiabatic electronic state ϕ_γ and vibrational states $\chi_{\gamma\mu}$ of the diatom, either H_2 or H_2^+

$$\psi(R, r, \rho_i) = \sum_{\gamma,\nu} F_{\gamma\nu}(R)\phi_\gamma(\rho_i|R, r)\chi_{\gamma\nu}(r), \quad (4)$$

where $F_{\gamma\nu}$ is the electronic scattering amplitude. Neglecting rotational modes of H_2 and H_2^+ and inserting expressions (2) and (4) into the Schrödinger equation, we arrive at a PSS scattering equation in the diabatic representation

$$\begin{aligned} &\{\nabla_R^2 + 2\mu_R[E - \varepsilon_{\gamma v}^d(R, \theta)]\}F_{\gamma v}(R, \theta) \\ &= 2\mu_R \sum_{\gamma'\neq\gamma}\sum_{v'} V_{\gamma v,\gamma' v'}^d F_{\gamma' v'}(R, \theta). \end{aligned} \quad (5)$$

In the infinite-order sudden approximation, the vibrationally resolved diabatic coupling matrix elements can be written as

$$\begin{aligned} &V_{\gamma v,\gamma' v'}^d(R, \theta) \\ &= \langle\chi_{\gamma v}(r)|V_{\gamma,\gamma'}^d(R, r, \theta)|\chi_{\gamma' v'}(r)\rangle, \end{aligned} \quad (6)$$

and the diabatic potential is given by

$$\varepsilon_{\gamma v}^d(R, \theta) = \varepsilon_\gamma^d(R, r_{\mathrm{e}}, \theta) + \Delta\varepsilon_r + \varepsilon_{\gamma v}, \quad (7)$$

where $\varepsilon_{\gamma\nu}$ is the pure, unperturbed vibrational excitation energy of the diatomic molecule. $V^d_{\gamma,\gamma'}(R,r,\theta)$ and $\varepsilon^d_\gamma(R,r,\theta)$ are obtained by a unitary transformation from the adiabatic to the diabatic representation.[21,22] As an example, the adiabatic potential energy curves for the geometries $r = 1.4\,a_0$ and $\theta = 45°$, $89°$ are shown in Fig.1(a) and the corresponding radial coupling matrix elements are shown in Fig.1(b). $\Delta\varepsilon_\gamma$ is a shift applied to the electronic diabatic energies to ensure the exact agreement with measurements in the separated-atom asymptotic limit $R \to \infty$. In order to solve F we introduce a partial-wave decomposition

$$F_{\gamma\nu}(R) = \sum_{lm} \frac{f_{\gamma\nu,lm}(R)}{R} \chi_{\gamma\nu}(r) Y_{lm}(\hat{R}), \tag{8}$$

where Y_{lm} are the spherical harmonic function. Inserting expression (7) into Eq.(5), we have the radial coupled equations

$$\left[\frac{\mathrm{d}^2}{\mathrm{d}R^2} - \frac{l(l+1)}{2\mu R^2}\right] f^{lm}_{\gamma\nu} - 2\mu \sum_{\gamma,\gamma'} V^d_{\gamma\nu,\gamma'\nu'}(R) f^{lm}_{\gamma'\nu'} + 2\mu E f^{lm}_{\gamma\nu} = 0. \tag{9}$$

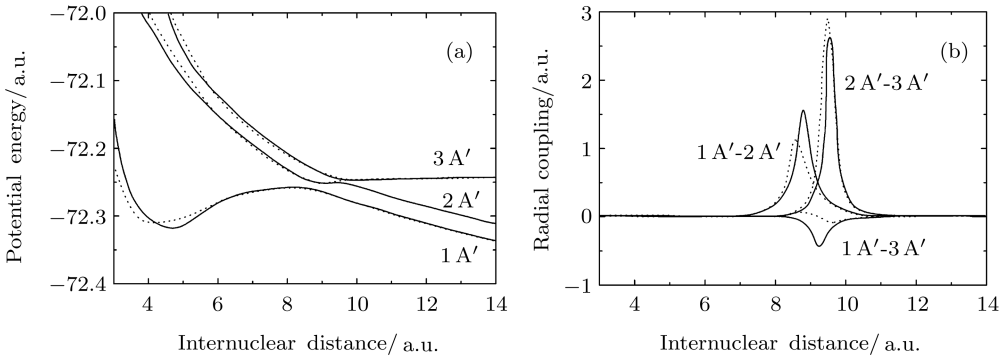


Fig.1. The adiabatic potential curves (a) and the radial couplings (b) for OH_2^{3+} as a function of R, with r fixed at $1.4\,a_0$, where solid curves refer to the case $\theta = 45°$ and dotted curves to the case $\theta = 89°$. In (a) the uppermost curves separate into $O^{3+}(2s^22p^2P^0) + H_2(X\ ^1\Sigma_g^+)$, the middle curves into $O^{2+}(2p3s\ ^2P^0) + H_2^+(X\ ^2\Sigma_g^+)$ and the lowest curves into $O^{2+}(2p3s\ ^3P^0) + H_2^+(X\ ^2\Sigma_g^+)$. In (b) the outermost couplings correspond to 2A′-3A′, the middle couplings to 1A′-3A′, and the innermost couplings to 1A′-2A′.

The radial functions satisfy the scattering boundary conditions

$$\lim_{R\to\infty} f^{lm}_{\gamma\nu}(R) \to \frac{1}{\sqrt{k_{\gamma'\nu'}}}\{\delta_{\gamma\nu,\gamma'\nu'} j_l(k_{\gamma\nu}R) + K^l_{\gamma\nu,\gamma'\nu'}\eta_l(k_{\gamma'\nu'}R)\},$$

with

$$k_{\gamma\nu} = \sqrt{2\mu[E - \varepsilon_{\gamma\nu\gamma\nu}(\infty)]}, \tag{10}$$

where j_l and η_l are the regular and the irregular Bessel–Ricatti functions, respectively; $k_{\gamma v}$ is the reduced momentum of the system; K^l is a real symmetric K matrix; the S matrix is given by

$$S^l = \frac{I + \mathrm{i}K^l}{I - \mathrm{i}K^l}, \tag{11}$$

with S^l being the S-matrix elements corresponding to lth partial wave. The cross section from the initial state i to the final state j is

$$\sigma_{i\to j} = \frac{\pi}{k_i^2} \sum_l (2l+1)|S^l|^2_{i,j}. \tag{12}$$

The differential cross sections are given by the expression

$$\frac{\mathrm{d}\sigma(\theta)}{\mathrm{d}\Omega} = \frac{1}{4k^2}\left[\sum_l (2l+1) S^l P_l(\cos\theta)\right]^2. \tag{13}$$

3. Results and discussion

It is known that there exist 19 vibrational bound states in $H_2^+(v')$, due to the computational capability, only 10 of 19 states were involved in the previous paper.[13] Therefore the convergence needs checking. A comparison between vibrationally state-selective cross sections for 10 and 19 states is presented in Table 1. For simplicity, only the results for capture to $O^{2+}(2p3s\ ^3P^0) + H_2^+$ at 10eV/u and $\theta = 45°$ are given. It can be seen that the higher vibrational states cause the redistribution of cross sections. But the summation over all vibrational states changes only a few percent, it is because it is difficult to excite the $H_2^+(v')$

Table 1. Vibrationally resolved state-selective cross sections for capture to $O^{2+}(2p3s\ ^3P^0) + H_2^+(v = 0{-}18)$ and $O^{2+}(2p3s\ ^3P^0) + H_2^+(v' = 0-8)$ at 10 eV/u and $\theta = 45°$.

	$O^{2+}(2p3s\ ^3P^0)$		$O^{2+}(2p3s\ ^3P^0)$
v=0	0.52757	v'=0	0.55396
v=1	0.83730	v'=1	0.88270
v=2	0.84944	v'=2	0.87556
v=3	0.75319	v'=3	0.75970
v=4	0.50496	v'=4	0.49258
v=5	0.29413	v'=5	0.25868
v=6	0.12060	v'=6	0.11021
v=7	0.03937	v'=7	0.03947
v=8	0.02132	v'=8	0.02256
v=9	0.01451	v'=9	
v=10	0.01281		
v=11	0.01260		
v=12	0.01369		
v=13	0.01582		
v=14	0.01803		
v=15	0.01829		
v=16	0.01593		
v=17	0.01047		
v=18	0.00339		

ions to the high vibrational states for the lower impact energies (< 10 eV/u), the cross sections are mainly distributed in the lower states ($v' < 5$). It is believed that the contributions from the high vibrational states of $H_2^+(v)$ will become more and more important as the projectile energy increases.[13,23] Therefore, in our calculations, the ground states of $O^{3+}(2s^22p\ ^2P^0)$ and $H_2(v = 0)$ are considered for the initial channel, while the excited states of $O^{2+}(2s^22p3s\ ^{1,3}P^0)$ and $H_2^+(v = 0 - 18)$ are included for the final channels. Totally, 39 coupled channels in Eq.(9) are solved, and much computational time is required due to a large number of partial waves appearing with the increase of impact energy. In the present work, the electronic and the vibrational state-selective differential cross sections for the lower energies of 0.1, 1.0 and 10 eV/u are calculated in two orientations of 45° and 89°.

The state-selective differential cross sections (DCSs) for captures to $O^{2+}(2p3s\ ^1P^0)$ and $O^{2+}(2p3s\ ^3P^0)$ are displayed in Fig.2. The orientation angle is 89°, and the impact energies are 0.1, 1.0 and 10.0 eV/u, respectively. The cross sections have been summed over all the vibrational states of $H_2^+(v')$. The DCSs show a similar behaviour: they decrease with the increase of scattering angle, and beyond a specific angle they oscillate with angle. We consider these oscillating structures resulting from the partial-wave interference in expression (12).[24–26] A comparison among the DCSs at different impact energies shows that with the increase of impact energy, the scattering probability becomes bigger at small angles. This is because high-speed collision makes the interaction time short, thus the energy and momentum transfers

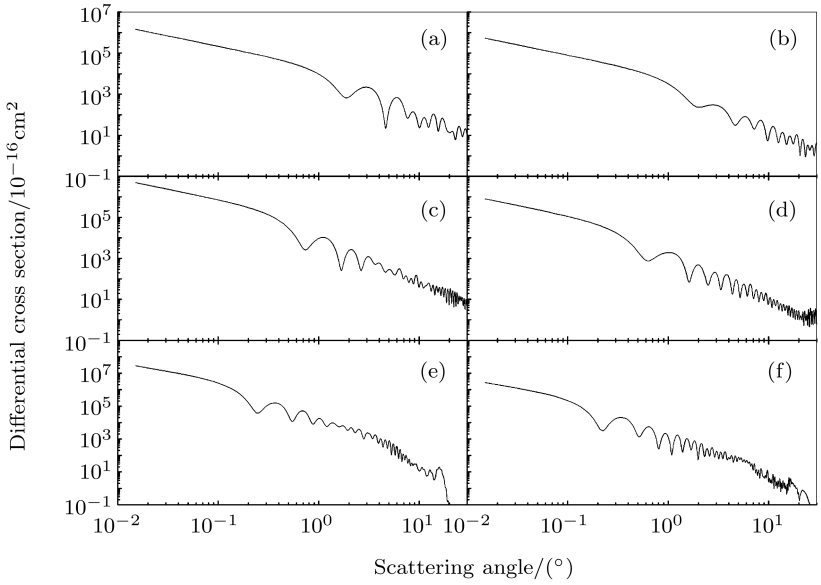


Fig.2. State-selective differential cross section for an orientation angle $\theta = 89°$ in O^{3+}-H_2 collisions, with captures to $O^{2+}(2p3s\ ^3P^0) + H_2^+(X^2\Sigma_g^+, v = 0-18)$ at 0.1 (a), 1.0 (c), and 10 eV/u (e), captures to $O^{2+}(2p3s\ ^1P^0) + H_2^+(X^2\Sigma_g^+, v = 0-18)$ at 0.1 (b), 1.0 (d) and 10 eV/u (f), the cross sections being summed over all the vibrational states of $H_2^+(v')$.

from projectile to target become smaller, the projectile is scattered at a smaller angle, which is similar to the case of "glancing collision".[27] Moreover, the specific angles at which the oscillations appear decrease in the form of $E_{\rm p}^{-1/2}$, which is consistent with the conservation of angle momentum in classical scatterings. For the same impact energy, the structures of differential cross section for capture to $O^{2+}(2p3s^3P^0)$ are similar to those for the case of $O^{2+}(2p3s^1P^0)$. This is due to the fact that the charge transfer process in collision mainly takes place at the avoided crossings of the potential curves. For this case, the positions of energy levels and avoided crossings for these two final states are very close to each other.[13]

For an orientation angle of 45°, the state-selective differential cross sections are plotted in Fig.3. Similar to the case at an orientation angle of 89°, the DCSs decrease with the increase of scattering angle, beyond a specific angle the oscillating behaviour appears although the decreasing tendency in DCSs still exists. Compared with the case at 89°, the values of DCSs are small, which is due to the small state-selective cross sections.[13]

A great number of vibrational state-selective differential cross section data are produced, and here we present two examples only. The vibrational state-selective DCSs for capture to $O^{2+}(2p3s\ ^3P^0) + H_2^+(v')$ are plotted in Fig.4. The impact energy is 1.0 eV/u, the orientation angle $\theta = 89°$, and $v' = 0$, 1, 2, 3. The vibrational state-selective DCSs decrease as the scattering angle increases, and the oscillating behaviour appears beyond a specific angle. A comparison among DCSs for capture to different values of v' shows that the DCS values are close to each other, but we can find that the angles for the first minimum in oscillating structures decrease with the increment of v', which means that the more momenta are required to be transferred when $H_2^+(v')$ is expected to be excited to higher vibrational states. For the vibrational state-selective cross sections capturing to $O^{2+}(2p3s\ ^1P^0)$ + $H_2^+(v')$, the DCSs show a similar behaviour to the above case, so the figure is not given here. Different from the case for capture to $O^{2+}(2p3s\ ^3P^0)$, the DCSs for capture to $O^{2+}(2p3s\ ^1P^0)$ decrease evidently as the vibrational quantum number v' increases. The cross section for charge transfer is mainly determined by the position of avoided crossing points and the coupling strengths between the adjacent channels, and both the position of avoided crossing point and the coupling strength will change as v' increases. But because so many channels are involved in our calculations, many direct and indirect processes are coupled together and, the reason why so is required to be given the further work.

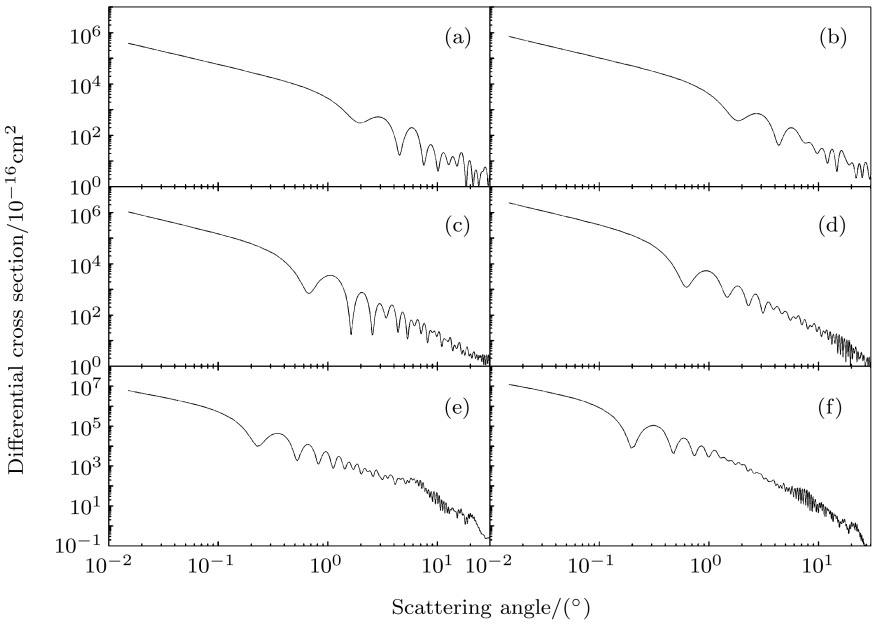


Fig.3. State-selective differential cross section for an orientation angle $\theta = 45°$ in O^{3+}-H_2 collisions with captures to $O^{2+}(2p3s\ ^3P^0) + H_2^+(X^2\Sigma_g^+, v = 0-18)$ at 0.1 (a), 1.0 (c), and 10 eV/u (e), captures to $O^{2+}(2p3s\ ^1P^0) + H_2^+(X^2\Sigma_g^+, v = 0-18)$ at 0.1 (b), 1.0 (d) and 10 eV/u (f), and the cross sections being summed over all the vibrational states of $H_2^+(v')$.

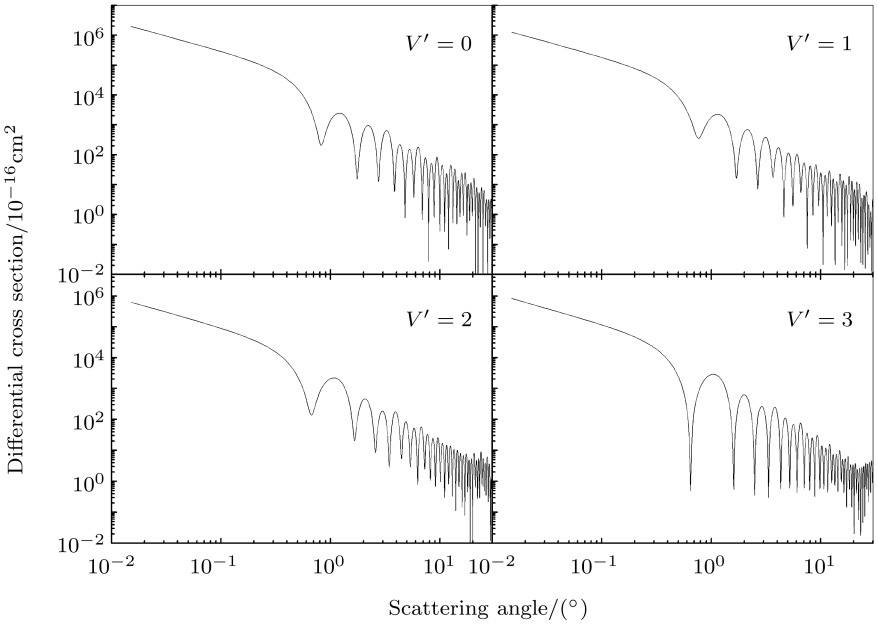


Fig.4. Vibrational state-selective differential cross sections for capture to $O^{2+}(2p3s\ ^3P^0)$ + $H_2^+(v')$ in O^{3+}–H_2 collisions with the impact energy being 1.0 eV/u, and the orientation angle $\theta = 89°$.

The vibrational state-selective differential cross sections for capture to $O^{2+}(2p3s\ ^3P^0)$ at an orientation angle $\theta = 45°$ are given in Fig.5. The impact energy is 1.0 eV/u, and $v' = 0$, 1, 2, 3. As is well known, the more information on collisional dynamics can be obtained from the differential cross sections. Especially, we may determine the orientations of molecules by identifying the vibrational state-selective differential scattering processes. As an attempt, we make a comparison between the vibrational state-selective DCSs for two orientation angles of 89° and 45° in Figs.4 and 5. It is easy to find that the DCS values are strongly orientation-dependent. For example, the DCS for capture to $O^{2+}(2p3s\ ^3P^0)$ + $H_2^+(v' = 1)$

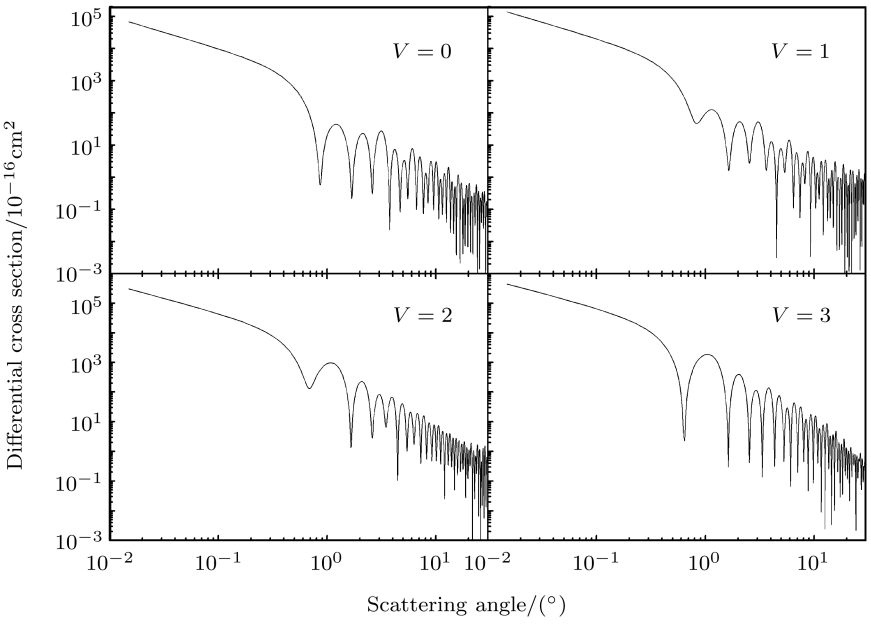


Fig.5. Vibrational state-selective differential cross sections for capture to $O^{2+}(2p3s\ ^3P^0)$ + $H_2^+(v')$ in O^{3+}–H_2 collisions with the impact energy being 1.0 eV/u, and the orientation angle $\alpha = 45°$.

at 89° in Fig.4 is about one order of magnitude higher than that at 45° in Fig.5. At low impact energies, the polarization interactions between projectile and target are essential to the charge transfer processes, and the dependence of polarization on H_2 molecular orientation may be the reason for the difference in DCS. Furthermore, after calculations we find that for capture to O^{2+} $(2p3s\ ^1P^0) + H_2^+(v')$ processes, the cross-section ratios for the values of v' at 89° and 45° are different, for example, the ratio of $\sigma(v'=1)/\ \sigma(v'=0) \approx 0.1$ at a small angle in the $\theta = 89°$ case. However, for the $\theta = 45°$ case, $\sigma(v'=1)/\sigma(v'=0) \approx 1$. Therefore, by using this orientation dependence, it is also possible to develop a new diagnostic method to determine the molecule orientations.

4. Conclusion

The quantum-mechanical molecular-orbital coupled-channel method is employed to study the non-dissociative charge transfer processes in O^{3+}–H_2 collisions. The orientation-dependent, electronic and vibrational state-selective differential cross sections at low energies ($< 10\,\mathrm{eV/u}$) are presented in the infinite order sudden approximation. It is found that the electronic and the vibrational state-selective differential cross sections have similar behaviours: they decrease with the increase of the scattering angle and beyond a specific angle the oscillating structures appear. Moreover, the strong orientation-dependence of the vibrational state-selective differential cross section is found, and the possibility to determine the orientations of molecule H_2 by identifying the vibrational state-selective differential scattering processes is discussed. Up to know, no experimental measurement on the differential cross sections has been performed for this system, therefore, the experiments are highly expected to check our results.

References

[1] Lepp S and McCray R 1983 *Astrophys. J.* **269** 560
[2] Cravens T E 1997 *Geophys. Res. Lett.* **24** 105
[3] Haberli M, Gombosi T I, De Zeeuw D L, Combi M R and Powell K G 1997 *Science* **276** 939
[4] Krasheninnikov S I, Pgarov A Yu and Sigmar D J 1996 *Phys. Lett.* A **214** 295
Krasheninnikov S I, Pgarov A Yu and Sigmar D J 1996 *Phys. Lett.* A **222** 251
[5] Janev R K, Kato T and Wang J G 2000 *Phys. Plasma* **7** 4364
[6] Elton R C, Cobble J A, Griem H R, Montgomery DS, Mancini R C, Jacobs V L and Behar E 2000 *EltonJ. Quant. Spectra. Radiat. Transf.* **65** 185
[7] Rosmej F B, Griem H R, Elton R C, Jacobs V L, Cobble J A, Faenov A Ya, Pikuz T A, Geißel M, Hoffmann D H H, Süß W, Uskov D B, Shevelko V P and Mancini R C 2002 *Phys. Rev.* E **66** 056402
[8] Elizaga D, Errea L F, Gorfinkiel J D, Illescas C, Méndez L, Macías A, Riera A, Rojas A, Kroneisen O J, Kirchner T, Lüdde H J, Henne A and Dreizler R M 1999 *J. Phys.* B **32** 857
[9] Bacchus-Montabonel M C 1999 *Phys. Rev.* A **59** 3569
[10] Errea L F, Macias A, Mendez L and Riera A 1999 *J. Phys.* B **32** 4065
[11] Errea L F, Gorfinkiel J D, Macias A, Mendez L and Riera A 1999 *J. Phys.* B **32** 1705
[12] Stancil P C, Zygelman B and Kirby K in *XX International Conference on the Physics of Electronic and Atomic Collisions* edited by Aumayr F, Betz G and Winter H P (Singapore: World Scientific) p537
[13] Wang J G, Stancil P C, Turner A R and Cooper D L 2004 *Phys. Rev.* A **69** 062702
[14] Wu Y, Liu L and Wang J G 2008 *Acta Phys. Sin.* **57** 947
[15] Crandall D H, Mallory M L and Kocher D C 1977 *Phys. Rev.* A **15** 61
[16] Phaneuf R A, Meyer F W and McKnight R H 1978 *Phys. Rev.* A **17** 534
[17] Meyer F W, Phaneuf R A, Kim H J, Hvelplund P and Stelson P H 1979 *Phys. Rev.* A **19** 515
[18] Phaneuf R A, Alvarez I, Meyer F W and Crandall D H 1982 *Phys. Rev.* A **26** 1892
[19] Afrosimov V V, Basalaev A A, Donets E D and Panov M N 1980 *JETP Lett.* **31** 600
[20] Church D A and Holzcsheiter H M 1989 *Phys. Rev.* A **40** 54
[21] Zygelman B, Cooper D L, Ford M J, Dalgarno A, Gerratt J and Raimondi M 1992 *Phys. Rev.* A **46** 3846
[22] Heil T G, Butler S E and Dalgarno A 1983 *Phys. Rev.* A **27** 2365
[23] Stancil P C, Wang J G, Turner A R and Cooper D L 2004 *Faraday Discussion* **127** 73
[24] Gao R S, Dutta C M, Lane N F, Smith K A, Stebbings R F and Kimura 1992 *Phys. Rev.* A **45** 6388
[25] Cabrera-Trujillo R, Ohrn Y, Deumens E, Sabin J R and Lindsay B G 2002 *Phys. Rew.* A **66** 042712
[26] Suno H, Rai S N, Liebermann H P, Buenker R J, Kimura M and Pichl L 2006 *Phys. Rev.* A **74** 012701
[27] Stolterfoht N, DuBois R D and Rivarola R D 1997 *Electron Emission in Heavy Ion-Atom Collisions* (Heidelberg: Springer) p11